Critical point symmetries in deformed odd-A nuclei

Yu Zhang, Feng Pan, Yu-Xin Liu, and J. P. Draayer

Phys. Rev. C **84**, 054319 — Published 22 November 2011

DOI: 10.1103/PhysRevC.84.054319

Critical point symmetries in deformed odd-A nuclei

Yu Zhang,[1] Feng Pan,[1,2] Yu-Xin Liu,[3,4] and J. P. Draayer[2]

[1]*Department of Physics, Liaoning Normal University, Dalian 116029, China*
[2]*Department of Physics and Astronomy, Louisiana State University, Baton Rouge, LA 70803-4001, USA*
[3]*Department of Physics and the National Key Laboratory of Nuclear Physics and Technology, Peking University, Beijing 100871, China*
[4]*Center of Theoretical Nuclear Physics, National Laboratory of Heavy Ion Accelerator, Lanzhou 730000, China*

A scheme that elucidates the nature of critical point symmetries in deformed odd-A nuclei by linking them to critical point symmetries of neighboring even-even nuclei is introduced. Specifically, a new symmetry, called SX(3), is advanced that shows primary characteristics of an assumed strong-coupling limit for odd-A systems. It is found that the SX(3) symmetry can be used to identify the soft collective structures in odd-A system. A preliminary application of the new scheme to describe the lowest positive parity bands of ^{193}Ir is also shown.

PACS numbers: 21.60.Fw, 21.60.Ev, 21.10.Re, 64.70.Tg

Critical point symmetries (CPS) [1–3] play an important role in understanding the evolution of nuclear collective structures in medium and heavy mass regions because they provide benchmark results for nuclei undergoing phase transitions [4]. Particularly, CPS can be used to provide parameter-free predictions of nuclear spectra, many having been confirmed by experiment [2, 3, 5, 6]. Since CPS have been observed in even-even nuclei, it is reasonable to extend the CPS concept to a description of odd-A systems. The first case, called E(5/4) [7], was introduced by Iachello to describe a γ-soft E(5) CPS coupled to a j=3/2 particle through a spin-orbit interaction. ^{135}Ba was suggested as an empirical example of the E(5/4) CPS. A detailed analysis of the agreements as well as the discrepancies between experimental results and theory was also reported [8]. Another case, called E(5/12) [9], was developed by Alonso, Arias, and Vitturi, when they extended the E(5/4) CPS case with a particle in the $j = 3/2$ orbit to a multi-j scheme with $j = 1/2,\ 3/2,\ 5/2$. Similarly, an X(5/2j+1) scheme [10] was proposed by coupling the X(5) core with a single-j particle.

These formulations are close in spirit to a weak-coupling picture, where the angular momentum of the collective core and that of the particle are both considered to be conserved quantities. Collective cores in odd-A nuclei, on the other hand, are often strongly deformed. As a consequence, the associated single-particle orbits can no longer be spherical. In such cases the particle-rotor model provides an alternative formulation [11], in which the core is assumed to be an axial-deformed rotor with the particle constrained to the field created by the core. Although collective rotation is also involved in the various CPS descriptions, the motion of the core is quite different from that of a rigid rotor described in the particle-rotor model. Actually, the collective core of nucleus described by the CPS models is characterized as soft or perhaps even as having a floppy shape in contrast to the rigid rotor description. Moreover, collective vibrations are also involved in the CPS, of which the spectrum thus become richer than that induced by a pure rotation. Similar situations in even-even systems have been discussed in detail within the collective model [12, 13] of Bohr and Mottelsson, the Variable Moment of Inertia (VMI) model [14], and so on. The purpose of this work is to provide a general CPS scheme in the strong-coupling limit for odd-A nuclei with the even-even core close to a critical point of a shape phase transition to explore whether or not such soft collective features confirmed in even-even nuclei show themselves in odd-A systems. The procedure outlined can be extended directly to odd-odd systems, which may be of interest as well.

To describe a deformed odd-A nucleus with an even-even core around the critical point of a shape phase transition, the Hamiltonian and wave function of a single valence particle may be expressed in the intrinsic frame of the deformed core described by the corresponding CPS. Thus, the Hamiltonian of the odd-A nucleus in the strong-coupling limit can be written as

$$H = H_{\rm CPS} + H_{\rm sp} \tag{1}$$

where $H_{\rm CPS}$ and $H_{\rm sp}$ are the Hamiltonian of the core and the single particle, respectively. It is assumed that there is no additional interaction between the core and the particle except that included in the strong-coupling limit itself [11]. It will be proven that analytical solutions of the model Hamiltonian (1) may be found with similar approximations to those used in the original CPS approach [1–3].

As a concrete example, we consider a core with the X(3) CPS [3], which can be regarded as the γ-rigid limit at the critical point of the spherical to axially deformed shape phase transition. In contrast to a rigid rotor, the X(3) CPS corresponds to a soft rotor. When the core is coupled with a spin j particle, the collective part in Eq (1) is given as $H_{\rm CPS} = H_{\rm X(3)}$, which is the Hamiltonian of the X(3) CPS. The total angular momentum of the odd-A nucleus may be expressed as $\hat{J} = \hat{L} + \hat{j}$, where $\hat{j}$ is the angular momentum operator of the single-particle, and $\hat{L}$ is that of the even-even core. The explicit Hamiltonian of the X(3) CPS [3] is shown as

$$H_{\rm X(3)} = -\frac{\hbar^2}{2B}\left[\frac{1}{\beta^2}\frac{\partial}{\partial\beta}\beta^2\frac{\partial}{\partial\beta} - \frac{1}{3(\beta\hbar)^2}\hat{L}^2\right] + V(\beta) \tag{2}$$

with

$$\hat{L}^2 = -\hbar^2\left[\frac{1}{\sin\theta}\frac{\partial}{\partial\theta}\sin\theta\frac{\partial}{\partial\theta} + \frac{1}{\sin^2\theta}\frac{\partial^2}{\partial\phi^2}\right] \tag{3}$$

and

$$V(\beta) = \begin{cases} 0, & \beta \le \beta_W, \\ \infty, & \beta > \beta_W. \end{cases} \quad (4)$$

As analyzed in [15], the potential at the critical point of the spherical-axially deformed shape phase transition in odd-A nuclei is rather flat for $\gamma = 0$, thus the square well $V(\beta)$ in (4) is adopted to describe the flat potential as used in the related even-even cases [1]. The single particle part may be taken as the Hamiltonian of the deformed-shell model [16] with

$$H_{\rm sp} = \sum_i E^i_{\Omega_i} f^\dagger_{i\Omega_i} f_{i\Omega_i}, \quad (5)$$

where $f^\dagger_{i\Omega_i}$ ($f_{i\Omega_i}$) is the creation (annihilation) operator of the valence particle in the i-th Nilsson orbit, and $E^i_{\Omega_i}$ is the corresponding single-particle energy. By using

$$\hat{L}^2 = (\hat{J}-\hat{j})^2 = \hat{J}^2 + \hat{j}^2 - 2(\hat{J}_z\hat{j}_z) - \hat{J}_+\hat{j}_- - \hat{J}_-\hat{j}_+, \quad (6)$$

where $j_\pm = \mp(j_x \pm i j_y)$, (1) can be regrouped as

$$H = H'_{\rm X(3)} + H_{\rm sp} + H' \quad (7)$$

with

$$H'_{\rm X(3)} = -\frac{\hbar^2}{2B}[\frac{1}{\beta^2}\frac{\partial}{\partial\beta}\beta^2\frac{\partial}{\partial\beta} - \frac{1}{3(\beta\hbar)^2}\hat{J}^2] + V(\beta), \quad (8)$$

and

$$H' = \frac{\hat{j}^2}{6B<\beta^2>} - \frac{2(\hat{J}_z\hat{j}_z) + \hat{J}_+\hat{j}_- + \hat{J}_-\hat{j}_+}{6B<\beta^2>}, \quad (9)$$

where $<\beta^2>$ is the average of β^2 over the eigenvector of (8). In the strong-coupling limit, H' is often neglected [11]. As a result, the Schrödinger equation $H\Psi = E\Psi$ can be separated into two parts: $H'_{\rm X(3)}\varphi(\beta,\theta_k) = E_\beta\varphi(\beta,\theta_k)$ with $\varphi(\beta,\theta_k)$=$\sqrt{\frac{2J+1}{8\pi^2}}\xi(\beta)D^J_{M,K}(\theta_k)$ and $H_{\rm sp}|\phi_{\Omega_i}\rangle = E^i_{\Omega_i}|\phi_{\Omega_i}\rangle$ with $j_z|\phi_{\Omega_i}\rangle = \Omega_i|\phi_{\Omega_i}\rangle$ if the single valence particle is in the i-th Nilsson orbit. Then, it is easy to get the total wave function $\Psi(\beta,\theta_k;\Omega_i) = \sqrt{\frac{2J+1}{8\pi^2}}\xi(\beta)D^J_{M,K}(\theta_k)|\phi_{\Omega_i}\rangle$ and the total energy $E = E_\beta + E^i_{\Omega_i}$. It should be noted that the potential in the X(3) CPS [3] is only a function of the β variable since the γ variable is frozen at $\gamma = 0$ representing the axial shape. The axial symmetry leads to the total angular momentum projected onto the intrinsic symmetric axis the same as that of the single particle with $K = \Omega_i$ because rotations around the symmetric axis of a quantum system are unobservable [11]. It is clear that the $H'_{\rm X(3)}$ describes the collective excitation, and $H_{\rm sp}$ describes the single-particle excitation. In odd-A nuclei, the head of a collective band is often determined by single-particle excitation, but intra-band structure is dominated by collective motion. The single-particle energy $E^i_{\Omega_i}$ in Eq. (5) is simply adjusted to accord with band heads determined in experiment. In the following, we will focus on the collective part described by $H'_{\rm X(3)}$. After introducing the reduced energies ε=$2BE_\beta/\hbar^2$ and reduced potentials u=$2BV/\hbar^2$, one can rewrite the Schrödinger equation, $H'_{\rm X(3)}\varphi(\beta,\theta_k) = E_\beta\varphi(\beta,\theta_k)$, by separating variable in the standard way

$$\hat{J}^2 D^J_{M,K}(\theta_k) = J(J+1)\hbar^2 D^J_{M,K}(\theta_k), \quad (10)$$

$$[-\frac{1}{\beta^2}\frac{\partial}{\partial\beta}\beta^2\frac{\partial}{\partial\beta} + \frac{1}{3\beta^2}J(J+1) + u(\beta)]\xi(\beta) = \varepsilon_\beta\xi(\beta). \quad (11)$$

Substituting $F(\beta) = \beta^{1/2}\xi(\beta)$ and $z = \beta\sqrt{\varepsilon_\beta}$, one can transform Eq. (11) inside the well into the Bessel equation

$$F'' + \frac{F\prime}{z} + [1 - \frac{\nu^2}{z^2}]F = 0, \quad (12)$$

where $\nu = \sqrt{\frac{J(J+1)}{3} + \frac{1}{4}}$. With the boundary condition $\xi(\beta_W) = 0$, one gets the eigenvalues $\varepsilon_{\beta;s,J} = (k_{s,J})^2$, $k_{s,J} = \frac{x_{s,J}}{\beta_W}$, where $x_{s,J}$ is the s-th zero of the Bessel function $J_\nu(k_{s,J}\beta)$. While the relevant eigenfunctions are given by $\xi_{s,J}(\beta) = c_{s,J}\beta^{-1/2}J_\nu(k_{s,J}\beta)$ with $c_{s,J}$ being the normalization constant determined by the condition $\int_0^{\beta_W}\xi^2_{s,J}(\beta)\beta^2 d\beta = 1$. As mentioned in [1], the Bessel functions with irrational order can be associated with projective representations of the E(n) group. The solution shown above are also relevant to the E(3) dynamical symmetry [17]. Finally, the total wave function should be symmetrized according to the axial symmetry as

$$\Psi(\beta,\theta_k;\eta) = \sqrt{\frac{2J+1}{16\pi^2}}\xi(\beta)[D^J_{M,K}(\theta_k)|\phi_K\rangle + (-)^{J+K}D^J_{M,-K}(\theta_k)|\phi_{\bar{K}}\rangle], \quad (13)$$

where η represents generically the coordinates of the single particle, and $|\phi_{\bar{K}}\rangle$ is the time-reversal state of $|\phi_K\rangle$. Since the Hamiltonian (7) is built from the core with the X(3) CPS coupled to a single particle in the strong-coupling limit, the corresponding CPS for odd-A nuclei is called SX(3).

B(E2) transition rates can be calculated by taking the quadrupole operator $T^{(E2)} = T_B + T_F$, where T_B acts only on the core and T_F acts only on the particle part. For simplicity, we only consider the term of T_B in this model, and its specific form is shown as

$$T_B = t\beta[D^2_{u,0}(\theta_k)\cos\gamma + \frac{1}{\sqrt{2}}(D^2_{u,2}(\theta_k) + D^2_{u,-2}(\theta_k))\sin\gamma], \quad (14)$$

where t is a scale factor. Thus, all B(E2) values are given in terms of only an overall scale, t. As mentioned above, the γ variable is frozen at zero so only the $D^2_{u,0}(\theta_k)$ term survives in (14), for which only the $\Delta K = 0$ transitions are allowed. In this approximation the B(E2) values are given by

$$B(E2;KsJ \to Ks'J') = \frac{1}{2J+1}|\langle Ks'J'||T_B||KsJ\rangle|^2. \quad (15)$$

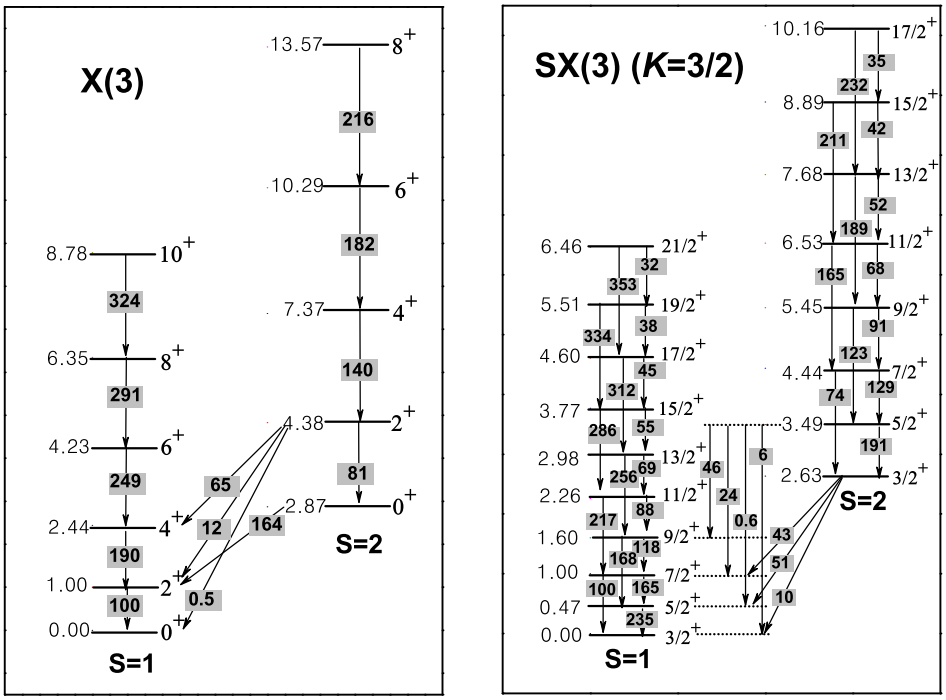

FIG. 1: Energy levels in the ground band (s=1) and β band (s=2) of the X(3) CPS [3] and those in the SX(3) CPS based on the $K = 3/2$ Nilsson single-particle level, normalized to the energy of the lowest excited $K+2$ state, together with $B(E2)$ transition rates, normalized to the transition $B(E2;(K+2)_1^+ \to K_1^+)$. It should be noted that $K = 0$ is taken for the even-even system described by the X(3) CPS, and only the transitions rates involved the lowest two states in the β band are shown as examples to illustrate the features of the interbands transition.

TABLE I: Typical energy ratios and B(E2) ratios in the X(3) and SX(3) CPS, where $K = 0$ is taken for the even-even system, and the results characterized by $\mathrm{SX(3)}_K$ are those calculated from the SX(3) CPS with $K = 1/2,\ 3/2,\ 5/2,\ 7/2$ and $9/2$.

	Even-Even	Odd-A				
CPS	X(3)	$\mathrm{SX(3)}_{1/2}$	$\mathrm{SX(3)}_{3/2}$	$\mathrm{SX(3)}_{5/2}$	$\mathrm{SX(3)}_{7/2}$	$\mathrm{SX(3)}_{9/2}$
$\frac{E_{(K+4)_1}-E_{K_1}}{E_{(K+2)_1}-E_{K_1}}$	2.44	2.34	2.26	2.22	2.19	2.17
$\frac{E_{(K+6)_1}-E_{K_1}}{E_{(K+2)_1}-E_{K_1}}$	4.23	3.98	3.77	3.65	3.57	3.51
$\frac{E_{K_2}-E_{K_1}}{E_{(K+2)_1}-E_{K_1}}$	2.87	2.68	2.63	2.67	2.72	2.78
$\frac{B(E2;(K+4)_1\to(K+2)_1)}{B(E2;(K+2)_1\to K_1)}$	1.90	1.85	2.17	2.52	2.82	3.08
$\frac{B(E2;K_2\to(K+2)_1)}{B(E2;(K+2)_1\to K_1)}$	1.64	0.88	0.43	0.28	0.20	0.15
$\frac{B(E2;(K+2)_2\to K_2)}{B(E2;(K+2)_1\to K_1)}$	0.81	0.77	0.74	0.73	0.73	0.73
$\frac{B(E2;K_2\to K_1)}{B(E2;(K+2)_1\to K_1)}$	0.00	0.00	0.10	0.21	0.30	0.39

By using the orthonormality condition $\langle\phi_{K'}|\phi_K\rangle = \delta_{KK'}$, Eq. (15) can be explicitly expressed as

$$B(E2;KsJ \to Ks'J') = t^2\langle JK20|J'K\rangle^2 I^2_{sJ;s'J'}\,, \qquad (16)$$

where

$$I_{sJ;s'J'} = \int_0^{\beta_W} \beta\xi_{s,J}(\beta)\xi_{s',J'}(\beta)\beta^2 d\beta\,. \qquad (17)$$

To show the spectral patterns of the SX(3) CPS, in the following, we consider the case based on the single-particle state with $K = 3/2$, namely the single valence particle is in a $K = 3/2$ Nilsson level. The results are shown in the right panel of Fig. 1. The spectral pattern of the X(3) CPS [3] is shown in the left panel of Fig. 1 in order to identify the similarities and differences of the criticality in odd-A and even-even systems since the SX(3) and X(3) CPS are proposed to describe the

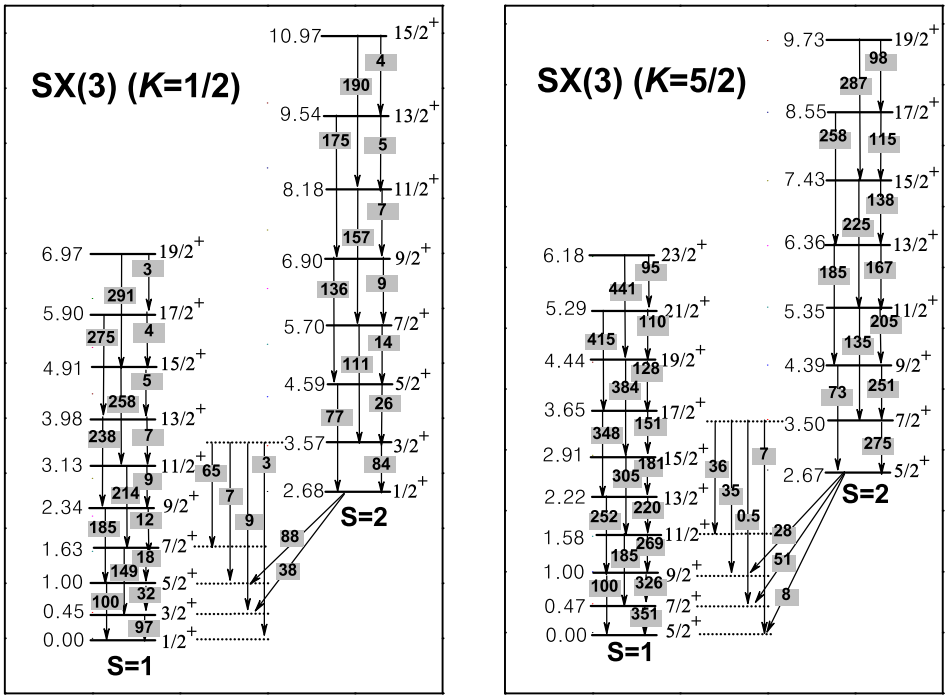

FIG. 2: The Same as those in Fig. 1 but for those of the SX(3) CPS based on the $K = 1/2$ and $K = 5/2$ single-particle level, respectively.

spherical to axially deformed shape phase transition in odd-A and even-even nuclei in this case, respectively. Moreover, in order to understand dynamic characters of the SX(3) CPS based on different single-particle levels, spectral patterns of the SX(3) CPS for $K = 1/2$ and $K = 5/2$ cases, and those for the $K = 7/2$ and $K = 9/2$ cases are shown in Fig. 2, and Fig. 3, respectively. It should be noted that both the energy levels and E2 transition rates are obtained analytically from the model only up to an overall scale factor.

As shown in the right panel of Fig. 1, the levels in each collective band in the SX(3) CPS form a rotational band with $\Delta J = 1$ for any two of adjacent levels in the band. As a result, the energy level density in the SX(3) symmetry should be much larger than that in the X(3) CPS, where $\Delta L = 2$ should be satisfied for adjacent levels within each collective band as shown in the left panel of Fig. 1. The predicted $B(E2)$ values in the SX(3) CPS with $\Delta J = 2$ are definitely larger than the ones with $\Delta J = 1$, except the lowest several transitions with comparable strength in each band. Moreover, the intraband $B(E2)$ values are generally larger than those of interband in the SX(3) CPS. The same situation is also observed in the X(3) CPS. All in all, the spectral structure in the SX(3) CPS is more complex than that in the X(3) CPS. In addition, single-particle excitations are often involved in the low-lying part of spectra in odd-A nuclei besides the collective rotational and vibrational excitations. As shown from Fig. 2 and Fig. 3, the collective spectra in the SX(3) CPS built on different single-particle states exhibit similar characters to the $K = 3/2$ case shown in Fig. 1, which only differ in band-head. However, the difference of the E2 transition rates with $\Delta J = 2$ and those with $\Delta J = 1$ gradually becomes small with the increasing of K as shown in Figs. 1-3.

Some typical quantities calculated from the SX(3) and X(3) CPS are presented in Table I in order to closely compare the specific features of the CPS in even-even and odd-A systems with different K. Since the order of the Bessel functions associated with the solutions of SX(3) CPS is different from that related with the X(3) CPS only by changing L for J, it is expected that the typical features provided with the X(3) CPS may also be observed in the SX(3) CPS, which is indeed shown by the typical energy ratios listed in Table I, where the energy ratios in the X(3) CPS vary little from those in the SX(3). However, $B(E2)$ ratios in the two cases are different. For example, $B(E2;K_2 \to K_1)$ is forbidden in the X(3) CPS and in the SX(3) CPS with $K = 1/2$, but the transition becomes allowed in the SX(3) CPS when $K > 1/2$. It is easily understood from Eq. (16) that the selection rule for the E2 transition is solely determined by the corresponding CG coefficients. While $\frac{B(E2;(K+2)_2 \to K_2)}{B(E2;(K+2)_1 \to K_1)}$ almost keeps unchanged in both even-even and odd-A systems as shown in Table I.

To further investigate the global characters of the related CPS, the collective rotational energies with different K in the

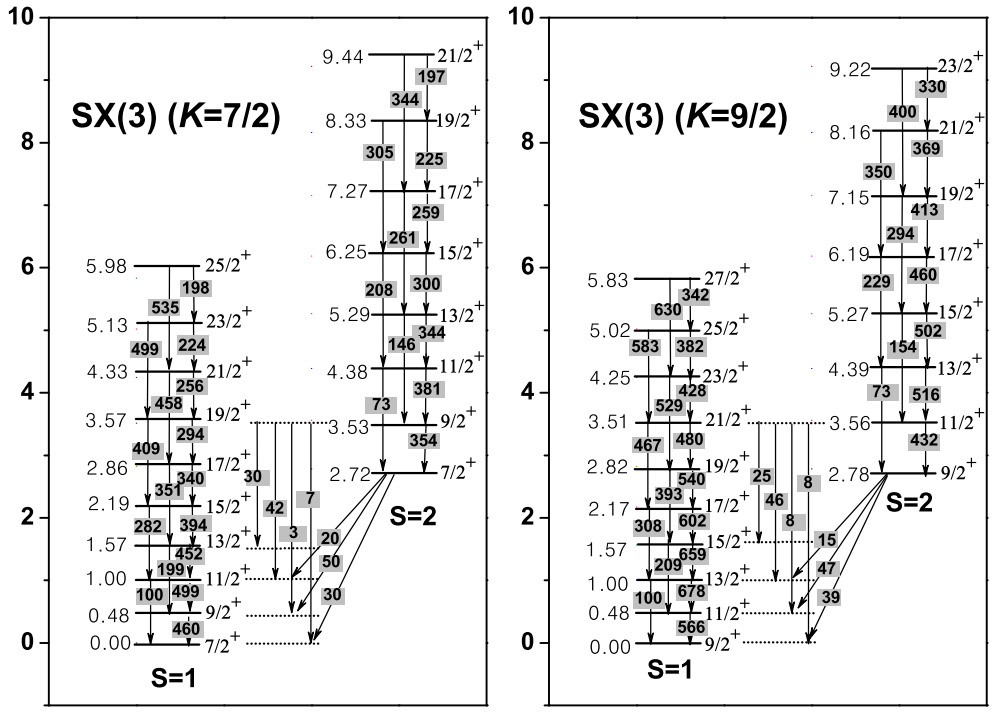

FIG. 3: The Same as those in Fig. 1 but for those of the SX(3) CPS based on the $K = 7/2$ and $K = 9/2$ single-particle level, respectively.

SX(3) CPS and those obtained from the $J(J+1)$ rule, which represents those of the rigid-rotor, together with the corresponding quantities calculated from even-even system, are shown in Fig. 4. It can be clearly seen from Fig. 4 that the SX(3) CPS plays a similar role in odd-A system as the X(3) CPS does in even-even system, namely the collective structures described by them are definitely soft. But the rigidity shown in the collective bands of the SX(3) will be enhanced with the increasing of K. Therefore, it is easier to identify the softness described by the SX(3) CPS in experiment when K is small. It should be emphasized that the SX(3) CPS is not a soft-core version of the particle-rotor model. The particle-rotor model only describes rotational motion based on single-particle excitations, while the collective β vibration is also involved in the SX(3) CPS as shown in Figs. 1-3. Because the γ variable has been frozen at $\gamma = 0$ in the SX(3) CPS, there is no γ vibrational motion involved. In order to describe γ vibrational modes, the X(3) core may be replaced by the X(5) core in Eq. (1), for which the potential related to the γ degree of freedom is assumed to be harmonic around $\gamma = 0$. The corresponding CPS in the strong-coupling limit may be called SX(5), which, however, is not a topic of this paper.

Some typical observables such those listed in Table I may be used to identify the experimental signals of the SX(3) CPS. Especially, the soft collective structure may be the most important indication of the SX(3) CPS. As a typical description of experimental results by the model, the lowest positive parity bands of ^{193}Ir, the ground band and the nearby band with $K = 1/2$, are taken to be fitted by the SX(3) CPS, which is shown in Fig. 5. According to the experimental assignments [18], the ground band $K = 3/2$ is built on the $\frac{3}{2}^+[402]$ Nilsson level, while the $K = 1/2$ band is built on the $\frac{1}{2}^+[400]$ Nilsson level [18]. The two collective bands involve most low-lying positive parity states of ^{193}Ir. As a comparison, the corresponding results calculated from the particle-rotor model (PRM) [11] are also shown in Fig. 5. It can be clearly seen from Fig. 5 that the experimentally observed energy levels in the ground band are described by the SX(3) CPS much better than those by the particle-rotor model. As for the $K = 1/2$ band, the spectrum in the experiment seems more rigid than that obtained from the SX(3) CPS but still softer than that described by the particle-rotor model. The experimental E2 transition rates among the states in the two positive parity bands are also taken to be compared with those calculated from the SX(3) CPS and the particle-rotor model. The results are listed in Table II. However, it can be observed from Table II that there is no obvious difference in the results of the E2 transition rates obtained from the two models, which both agree with the corresponding experimental data well. Therefore, the softness shown in the energy spectrum is the unique signal of the SX(3) CPS in this case. Other higher excited bands, for which multi-particle excitations may need to be considered in

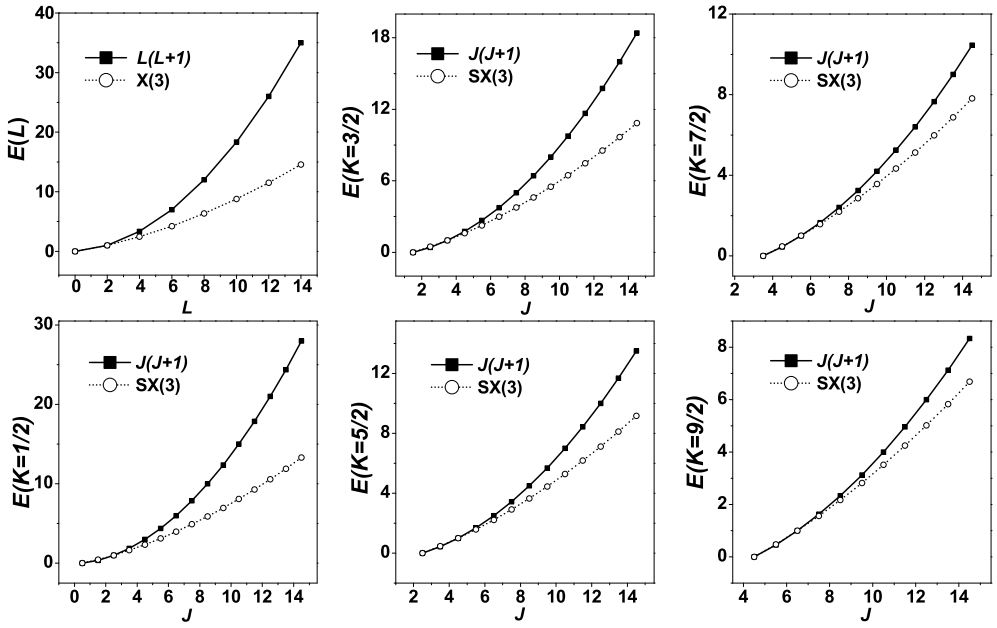

FIG. 4: Rotational energies in the ground band of the $X(3)$ CPS and the $L(L+1)$ rule in even-even system together with those in the SX(3) CPS and the $J(J+1)$ rules in odd-A system. All levels are normalized to the $L=2$ state for the even-even system, and the $J=K+2$ state for the odd-A system.

order to determine the position of band heads according to the deformed shell model, should display similar soft rotational feature. We conclude that the spectrum of ^{193}Ir displays its soft nature especially in the ground band, which can be described to some extent by the SX(3) CPS. It should be noted that the quantum number K assumed to be a good quantum number is only an approximation in the calculation even for the band-heads of the two bands of ^{193}Ir, in which there is no K-mixing mechanism considered with each band-heard being assigned by that of the specific Nilsson level according to the experiment [18]. Actually, ^{193}Ir was also discussed in other models previously [19–21], in which the asymmetry was considered in describing the rotational-like bands in ^{193}Ir. Therefore, further extension of the SX(3) CPS model to including the asymmetry may be needed in order to describe experimental results better. In addition, the interaction H' in Eq. (9), which leads to the K-mixing, can also be considered as done in the particle-rotor model [22]. But it is ignored in the present work because detailed calculation shows that it only changes the energy values of each level less than four percent for ^{193}Ir. Anyway, it seems that the SX(3) CPS can be taken as a better starting point than the particle-rotor model to describe the softness in the odd-A nuclei.

In summary, a general scheme for the description of CPS in the strong-coupling limit for odd-A nuclei is presented. The scheme provides a new way to investigate CPS driven collective modes in deformed odd-A systems. Moreover, the scheme outlined can also be used to study shape phase transitions in deformed odd-A nuclei with a corresponding CPS core in addition to the existing CPS models [7, 9, 10]. The SX(3) model is established as a specific example. It has been shown that the SX(3) CPS inherits the main characters of the corresponding CPS of the even-even core. As a typical application of the model, the first two positive parity bands of ^{193}Ir are taken to be fitted by the new CPS, and compared with the results obtained from the particle-rotor model. It is shown that the results of the new CPS theory agree with those of the experiment better than those obtained from the parti-

TABLE II: Experimentally observed intraband E2 transition rates for the $K=3/2$ and $K=1/2$ positive parity bands [18] of ^{193}Ir with those predicted from the SX(3) CPS and the particle-rotor model (PRM), where all the transition rates are normalized to $B(E2;7/2_1^+\to 3/2_1^+)$.

$J_i^\pi - J_f^\pi$	exp.	SX(3)	PRM	$J_i^\pi - J_f^\pi$	exp.	SX(3)	PRM
$7/2_1^+\to 3/2_1^+$	32	32	32	$11/2_1^+\to 7/2_1^+$	47	69	57
$7/2_1^+\to 5/2_1^+$	24	53	48	$3/2_2^+\to 1/2_1^+$	54	37	45
$5/2_1^+\to 3/2_1^+$	82	75	77	$5/2_2^+\to 1/2_1^+$	21	39	47
$9/2_1^+\to 5/2_1^+$	61	54	48	$5/2_2^+\to 3/2_2^+$	7	12	13

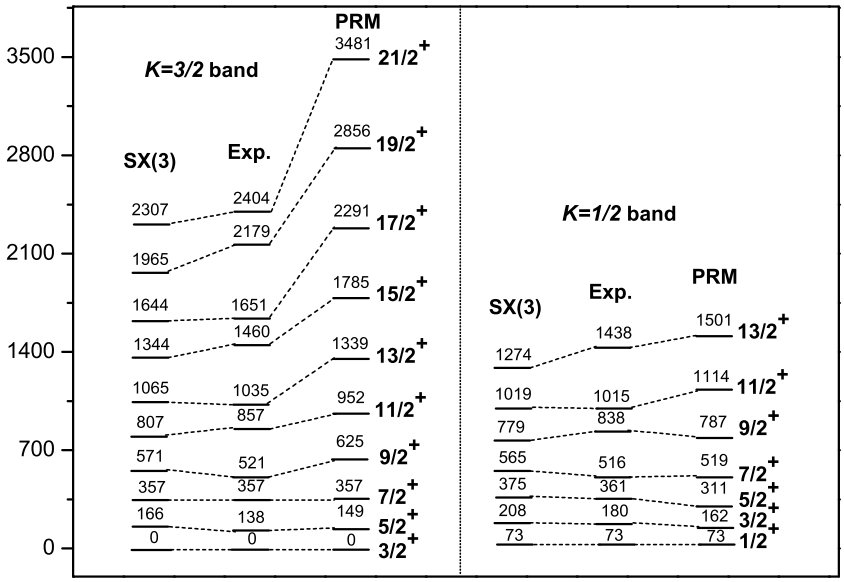

FIG. 5: Comparison of the experimental levels in the $K = 3/2$ ground band and $K = 1/2$ positive parity band [18] of ^{193}Ir with those calculated from the SX(3) CPS and the particle-rotor model (PRM), where all the levels are normalized to the first $7/2^+$ state, and the single-particle energy gap of the two bands is adjusted to accord with the band head observed in experiment.

cle plus rigid rotor model. Parallel studies in other algebraic models, such as the IBFM [15, 23, 24] should also be interesting. The strong-coupling scheme for the X(3) CPS can directly be extended to include multi-particle excitations, and also be applied to describe odd-odd systems, which can be treated as an even-even core coupled with a valence proton and a valence neutron. The scheme should also be applicable to other experimentally confirmed CPS [1–3], such as the X(5), Y(5), Z(5), and Z(4), which have been successfully used to elucidate various shape phase transitions in even-even nuclei. Finally, approximate analytical solutions of the CPS in the strong-coupling limit can always be realized as shown in the SX(3) CPS. Related study is in progress.

Support from the U.S. National Science Foundation (PHY-0500291 & OCI-0904874), the Southeastern Universities Research Association, the Natural Science Foundation of China (11005056, 11175078), the Doctoral Program Foundation of State Education Ministry of China (20102136110002), and the LSU–LNNU joint research program (9961) is acknowledged.

[1] F. Iachello, Phys. Rev. Lett. **85**, 3580 (2000); **87**, 052502 (2001); **91**, 132502 (2003).
[2] Dennis. Bonatsos, D. Lenis, D. Petrellis, and P. A. Terziev, Phys. Lett. B **588**, 172 (2004).
[3] Dennis. Bonatsos, D. Lenis, D. Petrellis, P. A. Terziev, and I. Yigitoglu, Phys. Lett. B **632**, 238 (2006); **621** 102 (2005).
[4] P. Cejnar, J. Jolie and R. F. Casten, Rev. Mod. Phys. **82**, 2155 (2010);
[5] R. F. Casten and N. V. Zamfir, Phys. Rev. Lett. **85**, 3584 (2000); **87**, 052503 (2001).
[6] R. M. Clark, et al., Phys. Rev. C **68**, 037301 (2003); **69**, 064322 (2004).
[7] F. Iachello, Phys. Rev. Lett. **95**, 052503 (2005).
[8] M. S. Fetea *et al*., Phys. Rev. **C 73**, 051301(R) (2006).
[9] C. E. Alonso, J. M. Arias, and A. Vitturi, Phys. Rev. Lett. **98**, 052501 (2007); Phy. Rev. **C 75**, 064316 (2007).
[10] Y. Zhang, F. Pan, Y. X. Liu, Z. F. Hou, and J. P. Draayer, Phys. Rev. **C 82**, 034327 (2010).
[11] W. Greiner and J. A. Maruhn, *Nuclears Models* (Springer-Verlag Berlin 1996).
[12] S. X. Harris, Phys. Rev. Lett. **13**, 663 (1964).
[13] F. X. Xu, C. S. Wu, and J. Y. Zeng, Phys. Rev. C, **40**, 2337 (1989).
[14] P. Holmberg and P. O. Lipas, Nucl. Phys. A **117**, 552 (1968).
[15] C. E. Alonso, J. M. Arias, L. Fortunato, and A. Vitturi, Phys.

Rev. **C 79**, 014306 (2009).
[16] S. G. Nilsson and I. Ragnarsson, Shapes and Shells in Nuclear Structure (Cambridge University Press, Cambridge, England, 1995).
[17] Y. Zhang, Z. F. Hou, ,Huan Chen, Haiqing Wei, and Y. X. Liu, Phys. Rev. **C 78**, 024314 (2008).
[18] E. Achterberg, *et al*., Nucl. Data Sheets **107**, 1 (2006).
[19] J. M. Arias, C. E. Alonso, and M. Lozano, Phys.Rev. **C 33**, 1482 (1986).
[20] F. K. McGowan, *et al*., Phys. Rev. **C 35**, 968 (1987).
[21] Ch. Vieu, *et al*., Z Phys. **A 290**, 301 (1979).
[22] M. E. Bunker and C. W. Reich, Rev. Mod. Phys. **43**, 348 (1971).
[23] J. Jolie, S. Heinze, P. Van Isacker, and R. F. Casten, Phys. Rev. **C 70**, 011305 (2004).
[24] C. E. Alonso, J. M. Arias, L. Fortunato, and A. Vitturi, Phys. Rev. **C 72**, 061302(R) (2005).